Supercritical CO2 Heat pump as an innovative solution for industrial applications above 150°C

Ali Mojtahed*, Gianluigi Lo Basso, Lorenzo Mario Pastore, Antonio Sgaramella, Livio de Santoli
Department of Astronautical, Electrical and Energy Engineering
Sapienza University of Rome, Rome, Italy
Email: ali.mojtahed@uniroma1.it

ABSTRACT

The term "industrial heat pump" refers to systems with outlet temperatures exceeding 100 °C. This paper introduces an innovative heat pump utilizing a reverse Brayton cycle, designed for high and very high temperature applications. Supercritical CO2 was selected as the working fluid due to its exceptional thermal properties. A thermodynamic model was developed in MATLAB Simulink. The energy performance of the machine was simulated and compared with available commercial models, particularly those using CO2 as a working fluid. The heat pump achieved a COP of up to 2.51 while generating saturated steam at 120 °C and is capable of producing saturated steam at a maximum temperature of 180 °C. An economic model is also developed. Sensitivity analysis was conducted to identify the most critical operational parameters from both energy and economic perspectives.

1 INTRODUCTION

The industry sector accounts for more than half of the energy consumption in the world. Based on International Energy Agency (IEA)(*IEA (2021),* data, in 2019, 57% of total electric energy consumption was dedicated to industrial processes yielding 9566 TWh. It makes the industry responsible for 9 Gt CO_2 emissions. The ambitious Net Zero Energy (NZE) scenario pathway proposed by IEA, by 2050 industry electrification will rise by 40%(*IEA, Industrial Energy Consumption by Fuel in the Net Zero Scenario,*). Accordingly, the total installed heat pump units for both space heating and industrial usage from 2021 to 2030 will be doubled and from 2030 to 2050 will double again.

The concept of high-temperature heat pump has been linked closely with the industry due to the available heat in this sector as a potential solution to reduce greenhouse gas emissions effect. Although the classification of temperature level is still not clear in the literature, all heat pump systems carry unique features to recover waste heat available during the industrial process. Such heat varies in the range of 30-80 °C which provides a valuable exergetic heat resource(Arpagaus et al., 2018). From the energy point of view, the classification of energy demand in the industry sector can be held based on the supply temperature requested in each application. Table 1 provides a classification of heat pump delivery temperature technologies used for the various industrial processes.

Table 1. Industrial heat pump temperature classification based on application("Future. Heat Pumps,"
2022)

Temperature range (°C)	Technology readiness level	Industrial Application
< 80	Commercialized	Paper: De-inking Food: Concentration Chemical Bio-reactions
80 - 100	Commercialized	Paper: Bleaching Food: Pasteurization Chemical: boiling
100: 140	Commercialized	Paper: drying Food: Evaporation Chemical: Concentration

https://doi.org/10.52202/077185-0181

140: 160	Pre-commercialized	Paper: Pulp boiling Food: Drying Chemical: Distillation Other: Steam production
160: 200	Small-scale	High temperature steam production
> 200	R&D	High temperature processes

As of today, more than half of industrial heat demand is characterized by heat delivery up to 400 °C which mostly is provided by fossil fuel boilers. The main heat consumers are chemical, food and paper manufacturers. Actual commercial heat pump units are capable of supplying heat at 150 °C. Such a threshold would be sufficient to meet around 30% of heat demand to substitute natural gas boilers avoiding 20 bcm (billions cubic meters) emissions ("Future. Heat Pumps," 2022).
Heat pumps present higher energy performance (COP >1) compared with combustion systems (η<1). Adding to that, rising penalization cost for CO_2 particularly in Europe, makes heat pumps a good candidate for industrial applications. Simple vapor compression cycles and absorption heat pumps due to historical background remain the most used technologies in the benchmark (Van de Bor & Infante Ferreira, 2013). The average delivery temperature reported in the literature for single stage vapor compression systems are in the range of 100-120°C (Jiang et al., 2022). The most mature technology are capable of lifting up the temperature by 30°C. However, recent works tend to push the barrier to go beyond current limit. Several studies have reported temperature lift of 40,50,60 and even 70 degrees(Ahmadi et al., 2016; Kabat et al., 2023; Patel & Raja, 2019).
CO_2 is one of the first natural refrigerants used as the working fluid in the world of refrigeration. Its thermodynamic properties specifically its high working pressure and fluid density facilitate the fabrication of light heat pump systems for a specific power consumption (M. H. Kim et al., 2004).In addition, a low compression ratio in CO_2 systems results in higher isentropic efficiency. Due to the low critical point of CO_2 (31.1 °C and 73.8 bar) it is convenient to use it in a trans-critical cycle. In this case the CO_2 surpass the critical point after the compression stage and it is known as trans-critical CO_2 heat pumps. However, the main issue with these systems is the high irreversibility caused during the expansion valve which results in COP drop(Yang et al., 2016). Several research works have tried to overcome this defect. One practical solution is to add an internal thermal recovery sector that can boost the performance of the machine. (Chen & Gu, 2005; S. G. Kim et al., 2005; Rony et al., 2019).
The maximum reported output temperature using an internal heat exchanger is 90 °C with COP over 3.0 (Cao et al., 2020; Lo Basso et al., 2020). Zhu et.al. improved the COP to 4.6 by applying the ejector to the expander (Y. Zhu et al., 2018). In another study (Lo Basso et al., 2023) authors reported a COP of 6.5 by forming a close loop for the external fluid circulating between the gas cooler and evaporator. In the trans-critical CO_2 cycle, the performance of the machine is strongly reduced by increasing the pressure ratio between the up and bottom stream pressure.
There is another potential configuration to utilize CO_2 entirely over the critical zone. (Zühlsdorf et al. 2019). In this case, a pressure ratio higher than before is required.
Having mentioned that, the current work investigates the performance of the reverse cycle sCO_2 heat pump. In contrast with the trans-critical cycle that is characterized by a low-pressure ratio and internal heat recovery to boost performance, the proposed layout features a high-pressure ratio to improve the output temperature profile without any thermal recovery sector. Instead, the expansion valve is replaced with an expansion device that generates mechanical work.
The main objective is to optimize and analyze the energy performance to generate high-value temperatures. After creating the mathematical model of each component, the main operational parameters would be recognized and discussed to optimize the performance. In the end, the economic model will be also presented.

https://doi.org/10.52202/077185-0181

Table 2: Close loop heat pump commercial models

Manufacture	series	Max. COP	Supply T	Heat source T	Capacity (kW)	Compressor Type	Refrigrant
Cobe Steel	SGH 165	3.0	135- 175	35-70	70-660	Twin screw	R245fa+ R134a
Vicking Heating Engines AS	HeatBooster S4		165	120	200	Piston	varies
Mitsubishi	QAHV		Ambient air	90	40-640	Inverter scroll	R744
Mayekawa	Eco sirocco	5.5	40	60:120	100	Reciprocating	R744
Johnson controls	Heat Pac	4.4	70	90	300:2000	Reciprocating	ammonia

2 Methodology

2.1 Super-critical CO_2 thermodynamic cycle

Figure 1 illustrates the P-h diagram of the proposed thermodynamic loop of the super-critical CO_2 heat pump. From this point of view, there is a distinct difference between the supercritical HP cycle and conventional vapor compression. The main difference occurs during the heat transfer that takes place in the forms of latent heat in the evaporator and condenser inside the conventional heat pumps. However, in the super-critical state, the working fluid experiences no phase change and remain entirely in the gaseous state. As a result, the evaporator and condenser are replaced with 'gas heater' and 'gas cooler' respectively. As it can be followed from Figure 1, the design parameters are set to ensure the cycle always above the critical point. As a result, the P_4> 75 bar and T_4 > 31 °C to remain in gaseous phase. One of the main issues reported in literature regarding trans critical CO_2 heat pump systems, scaling up the delivery temperature requires the higher pressure difference that increases throttle irreversible losses in the expansion phase. As a result of that effect, the COP tend to decrease (Y. Zhu et al., 2018). This phenomena occurs due the severe enthalpy changes near critical point (Rony et al., 2019). According to experimental data, when the temperature lift is above 100 °C, due to the thermodynamic limits, the performance of the machine shrink by 50%. This results in COP below 2.0(Yan et al., 2021). In order to avoid COP drop, this work proposes the mechanical useful work recovery from the expansion process and use it to feed the compressor.

https://doi.org/10.52202/077185-0181

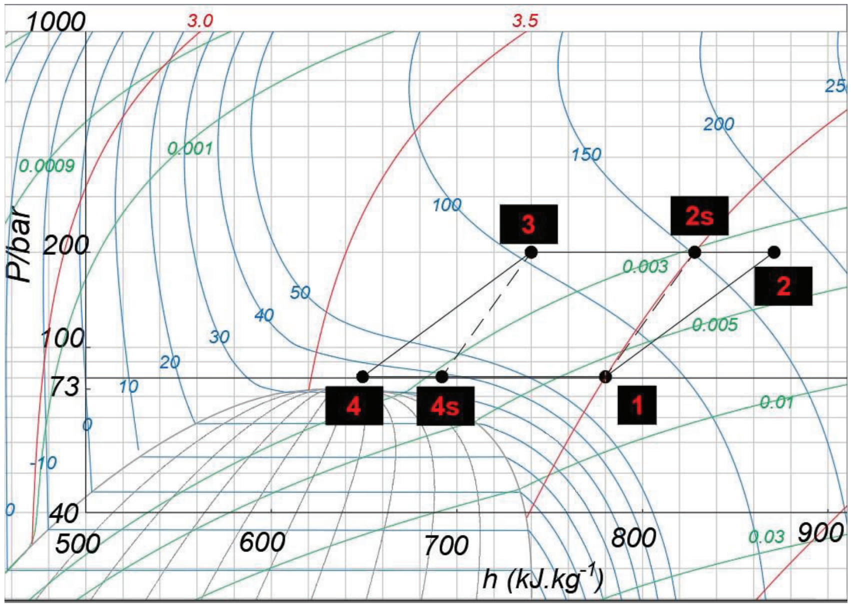

Figure 1: p-h diagram of the thermodynamic sCO2 Cycle, the original diagram is brought from Imperial College London 2012, reference state: h = 733.63 kJ/kg and s = 4.26 kJ/kg°C, for the gas at triple point (T = -56.558°C, and P = 5.1795 bar)

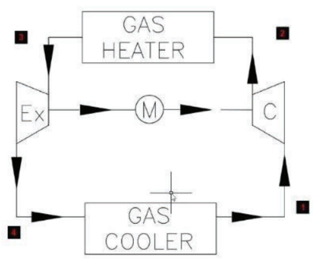

Figure 2: Presented layout.

2.2 Thermodynamic and Simulation model

The thermodynamic loop of sCO_2 heat pump is similar to the reverse Bryton cycle. In the P-h diagram brought in Figure 1, cycle 1-2-3-4-1 represents an irreversible real cycle while 1-2s3-4s is the ideal endo-reversible one. The isentropic efficiency of compression and expansion can be described as (Ahmadi et al., 2016; Bi et al., 2010):

$$\eta_{compression} = \frac{T_{2s} - T_1}{T_2 - T_1} \tag{1}$$

$$\eta_{expanssion} = \frac{T_3 - T_{4s}}{T_3 - T_4} \tag{2}$$

Where $\eta_{is,com}$ <1 and $\eta_{is,ex}$ <1 always are satisfied.

The total heat needed to be supplied by the heat pump can be derived as equation 4:

$$Q_{total} = Q_{subcooling} + Q_{saturation} + Q_{superheatig} \tag{4}$$

In equation 4, the total heat power involves three terms of the subcooling process, phase change and superheating. The subcooling process takes place by exchanging sensible heat between CO_2 and water up to the saturation point. This step occurs inside an economizer. After that, the saturated water enters the so-called evaporator undergoing a latent heat transfer. To ensure saturated steam at the delivery point, 5 °C of superheating is also applied to the steam profile. Equations 5 to 7 describe the expression for three main heat-exchanging processes:

https://doi.org/10.52202/077185-0181

$$Q_{subcooling} = \dot{m}_{water} \times (h_{sat\_l} - h_{in\_water}) \quad (5)$$
$$Q_{saturation} = \dot{m}_{water} \times (h_{sat\_s} - h_{sat\_l}) \quad (6)$$
$$Q_{superheating} = \dot{m}_{water} \times (h_{sat_s+5} - h_{sat\_s}) \quad (7)$$

In practice, in a similar way to heat recovery steam generator plants, to avoid the formation of bubbles inside the economizer which can block the flow rate (choking), a margin of at least 5 °C below the saturation point is considered. Hence equations 5 and 6 can be rewritten :

$$Q_{subcooling} = \dot{m}_{water} \times (h_{sat_l-°5} - h_{in\_water}) \quad (8)$$
$$Q_{saturation} = \dot{m}_{water} \times (h_{sat_s} - h_{sat_{l-°5}}) \quad (9)$$

The heat transfer process for the sCO_2 requires additional evaluation since the T-h diagram over the critical states does not have a linear distribution. In this case, the thermodynamic properties of CO_2 must be checked at each stage of the process to conserve the second law. Dividing the total heat transfer into the economizer and evaporator, each process can be divided and solved in N-finite iteration loop.

$$Q\_evap = \dot{m}_{water} \times [(h_{sat_s} - h_{sat_{l-°5}}) + (h_{sat_s+5} - h_{sat_s})] \quad (10)$$
$$Q\_evap = \sum_{i=0}^{N} \dot{m}_{CO2} \times ({h^i}_2 - {h^i}_1) \quad (11)$$
$$dQ\_ = Q\_evap / N \quad (12)$$

In equation 11, h^i_1 represents the inlet condition at each step, while h^i_2 is the outlet condition at each step. To solve the equation 11, 2 initial conditions are needed to be applied. The inlet condition of sCO_2, is obtained from the outlet compressor profile so :

$$T^0_1 = T_{CO2\_out\_compressor} \quad (13)$$

The outlet temperature of CO_2 can be calculated by fixing the pinch point from the steam profile to make sure that the two fluids diagrams are not cross over each other:

$$T^N_2 = T_{sat\_water} + T_{pinch} \quad (14)$$

For gaseous working fluid exchanging with water inside a shell and tube heat exchanger, a pinch point equal to 5 °C is assumed. (Zühlsdorf et al. 2019).
By knowing the temperature profile, the enthalpy values can be obtained and equation 11 would be solved. After solving the equation at each step, the enthalpy values would be updated to start another iteration.
For i = 0:N
$h_2^i = h_1^i - dQ/\dot{m}_{CO2}$
$h_2^i = h_1^{i+1}$
The same approach is applied to the economizer. In this case, the outlet temperature of sCO_2 will be obtained by solving the same equations. Equations 10:13 can be rewritten for economizer as:

$$Q\_eco = \dot{m}_{water} \times [(h_{sat_l-°5} - h_{in\_water})] \quad (15)$$
$$Q\_eco = \sum_{i=0}^{N} \dot{m}_{CO2} \times ({h^i}_2 - {h^i}_1) \quad (16)$$
$$dQ\_ = Q\_eco / N \quad (17)$$
$$T^0_1 = T_{out\_evap} \quad (18)$$

https://doi.org/10.52202/077185-0181

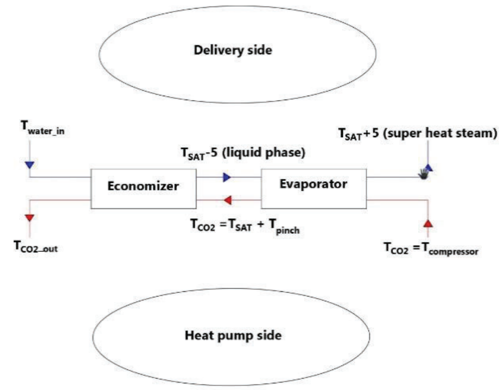

Figure 3: Schematic of the heat transfer process between water and sCO_2

After completing the temperature profile of both fluids,to evaluate the sufficient surface of the heat exchangers the logarithmic mean temperature difference (LMTD) is conducted:

$$Q_H = FAU_H \cdot LMTD \tag{19}$$

Where F is the correction factor depending on the geometry
LMTD is defined as logarithmic mean temperature difference.

$$LMTD = \frac{\Delta T_1 - \Delta T_2}{\ln\frac{\Delta T_1}{\Delta T_2}} \tag{20}$$

$$\Delta T_1 = T_{in\_hot} - T_{out\_cold} \tag{21}$$

$$\Delta T_2 = T_{out\_hot} - T_{in\_cold} \tag{22}$$

The compression and expansion work is calculated from an ideal isentropic adiabatic process that implies:

$$\frac{T_{2s}}{T_1} = \left(\frac{P_2}{P_1}\right)^{\frac{\gamma-1}{\gamma}} \tag{23}$$

The real COP can be evaluated by the ratio of actual delivery heat over the power consumption of the machine:

$$COP_{real} = \frac{Q_H}{W} \tag{24}$$

W in equation 24 represents the overall work that is derived from both the compressor and expansion device. It can be described also as equation 25:

$$COP_{real} = \frac{Q_H}{(W_{co} - W_{ex}).\eta_{motor}.\eta_{shaft}} \tag{25}$$

Where W_{com} is compressor work and W_{ex} is expansion device generated work that can be calculated by recalling Figure 1:

$$W_{com} = (h_2 - h_1) \times \dot{m}_{CO2} \tag{26}$$

$$W_{com} = (h_3 - h_4) \times \dot{m}_{CO2} \tag{27}$$

2.3 Industrial application

Saturated steam has various applications in different sectors of the industry. As a consequence, the application of a high-temperature heat pump to generate steam at the requested condition can be evaluated. The paper industry is one of the sectors that use steam for drying, textile and stripping purposes at the atmospheric pressure range of 2-16 bar and temperature of 120-200 °C. In the food industry, steam at 1-3 bar with a temperature profile in the range of 60-100 °C used in the pasteurization process. however, for evaporation steam at a maximum of 1 atmospheric bar at T =

https://doi.org/10.52202/077185-0181

40:80 °C would be enough. Industrial steam cleaners typically operate at 4-8 bar with 100-180 °C temperature profile. Finally in mining industry the heap leaching process require steam at atmosphere pressure and temperature range around 100-150°C.

Table 4: Application of steam in industry sectors

Application	Atmospheric Pressure (bar)	Temperature (°C)
Paper: drying	2-16	120-200
Paper: Textile	1-6	100-160
Paper: steam stripping	1-6	100-150
Food: Pasteurization	1-3	60-100
Food: evaporation	0.2-1	40-80
Mining: heap leaching	1	100-150
Chemical reactions	1-5	50-250
Steam cleaning	4-8	100-180

2.4 Economic model

The economic model for CO_2 heat pump with reverse Bryton cycle is estimated from the available studies in the literature (Zühlsdorf et al. 2019), (Huang et al. 2022). The capital cost of each component without assuming auxiliary equipment, engineering and labour work is reported in equation 29(Turton 2013):

$$\text{Log}\,(C_P^0) = k_1 + k_2 \log(X) + k_3 (\log(X))^2 \qquad (28)$$

In equation 29, X is the scaling parameter that determines the final cost (e.g for compressor the mechanical work , for heat exchanger the useful surface).

The complete version of equation 29 can be found in equation 30, featuring f_{BM} as the factor for engineering and labour work and auxiliary equipment; f_P as the pressure factor for heat exchanger construction; f_M as the additional cost for design of equipment in different materials(Ulrich, Vasudevan, and Ulrich 2004); and finally f_{CEPCI} which represents cost function in different years from the reference chosen year which was based on chemical engineering plant cost index (CEPCI) in 2017.

$$C_{BM} = f_{BM}.\, f_P.f_{CEPCI}\,.C_P^0 \qquad (29)$$

The values assumed for k1, k2, k3 and factors are reported in Table 5.

Table 5: parameter assumed for economic model

Component	Overall factor	K1	K2	K3
centrifugal compressor 1	541.7	2.2897	1.3604	-0.1027
centrifugal compressor 2	541.7	2.2897	1.3604	-0.1027
shaft	1	1.956	1.7142	-0.2282
shell and tube HE	200	3.2476	0.2264	0.0953
turbine radial	541.7	2.2476	1.4965	-0.1618
Piping	0.0025			

The main assumptions and technical considerations for simulation part can be seen in Table 6

https://doi.org/10.52202/077185-0181

Table 6: Technical assumption

Design parameter	Value	Unit
Heat source available	80	°C
η_{iso}	%78	-
ε_{HEX}	0.7	
ε_{motor}	0.98	
ε_{shaft}	0.98	
$U_{HEX\_liquid\_gas}$	40	W/m^2/K
$U_{HEX\_gas\_gas}$	40	W/m^2/K
$U_{HEX\_gas\_evap}$	42.5	W/m^2/K
Heat sink size	75	kW
T_{input_water}	20	°C
P_{low_HP}	75	bar
η_{com}	65%	

3 Results and discussion

3.1 COP and Capital cost

The simulation is carried out to evaluate the capacity of sCO_2 HP to generate saturated steam according to potential industrial applications. Consequently temperature profile in the range of 120 °C up to 185 °C is considered. The highest obtained COP is equal to 2.51 which diminishes by raising the delivery temperature to the minimum value of 1.57. The capital cost of the system on the other hand, there varies in the range of 114 k€ to 145 k€. For a steam profile below 150 °C, only one compression step is required. As it can be seen also in Figure 4 from 150°C so on, there is a shift in capital cost that belongs to the cost of the secondary compressor. By increasing the discharge pressure for a fixed saturation pressure, the temperature profile of CO_2 will be escalated as well. As a result, according to the total energy balance, the mass flow rate of CO_2 diminishes. This reduces the size of both expander and compressor which corresponds to more than half of total investment costs. In the other hand, with less mass flow rate on the CO_2 side, the heat transfer process requires more heat exchanger space. Eventually the heat exchanger price rises. Figure 5 illustrates the impact of pressure soaring on the final price for saturation pressure of 3 bar. As the pressure increases the overall distribution of main component tends to reduce the final cost. The total cost function reaches its minimum value at $P_{discharge}$ = 280 bar. After this point, the heat exchanger raising trend outweighs the turbo machinery part and determines the form of investment function.

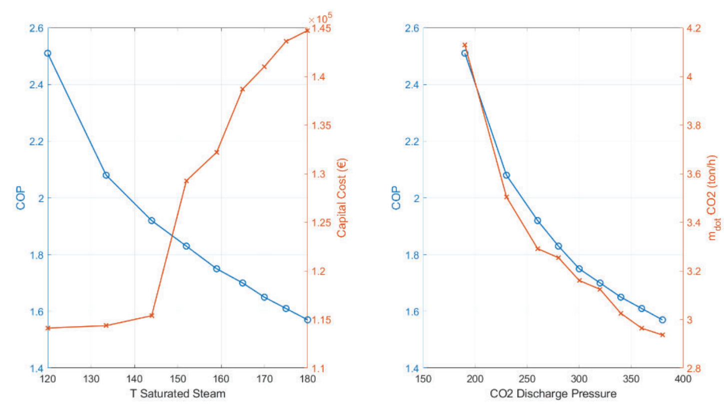

Figure 4: a) Steam temperature vs COP and capital cost; b) the impact of discharge pressure on COP and mass flow rate

https://doi.org/10.52202/077185-0181

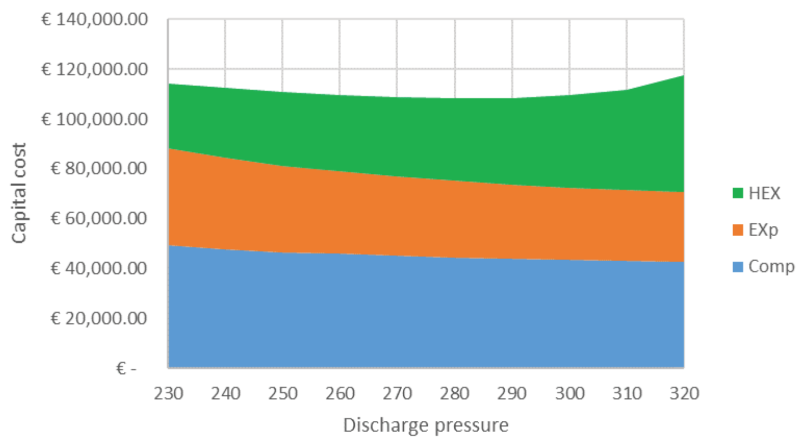

Figure 5 The impact of pressure rise on price distribution for $P_{saturated}$ = 3 bar

3.2 Pinch point

One of the main practical challenges in dealing with super critical CO_2, is the heat transfer process that mostly takes place between two fluids in the gaseous state. A complex heat exchanger design and huge surface are the main challenges that could reduce the heat exchanger effectiveness. The impact of pinch point variation on the overall performance of the machine and the heat exchanger surface is studied. By increasing the pinch point between CO_2 and the steam, the total surface of heat exchangers (economizer and evaporator) tends to decrease. Rising up the pinch point from 5 °C to 15 °C, the total effective surface for economizer and evaporator reduces by 27% and 21% respectively. This, however, surges the demand for higher $\dot{m_{CO2}}$ rate by 31%. As a consequence, the size of the compressor and the expansion device might be escalated which alters the COP. The simulation results suggest that the overall effect of pinch rise improves slightly the performance of the HP.

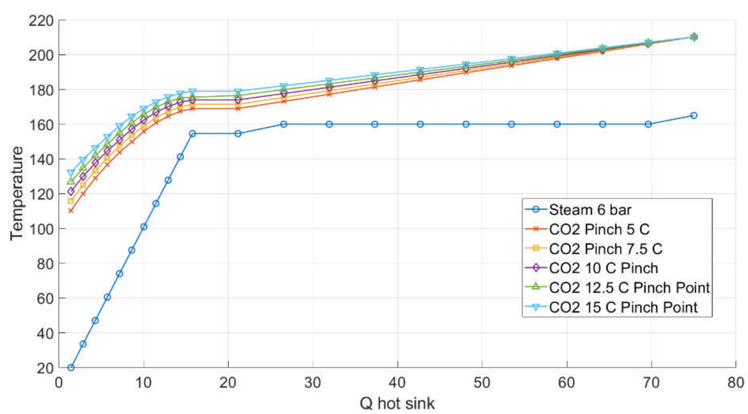

Figure 5: The effect of pinch point on the heat transfer process, Saturated steam at 6 bar

Table 7: variation of sCO2 parameters by pinch point

Pinch point	5	7.5	10	12.5	15
COP	1.75	1.76	1.77	1.78	1.79
A (m^2)	628	586	552	522	497
$\dot{m_{CO2}}$ $(tons/h)$	3160	3364	3597	3864	4173

https://doi.org/10.52202/077185-0181

3.3 Discharge pressure

Another design parameter that impacts the performance of the heat pump is discharge pressure. According to the isentropic process brought in equation 24, pressure increase results in temperature scale-up inside the compressor. This enlarges of course the specific work of the compressor. However, the CO_2 mass flow rate can be less than before;. This flow rate is determined by performing energy balance inside the evaporator. As a result, the overall mechanical work which is defined as the algebraic sum of compressor and expansion work must be recalculated. (In equation 27 and 28 both $\dot{m}$ and Δh change).

As illustrated in Figure 6, by increasing the discharge pressure, the overall work required to insert to the system reaches its maximum point and after that decreases again. This phenomenon occurs due to nonlinear characteristics of sCO_2 that imply uneven Δh distribution at different discharge pressures The maximum point representing the highest difference between compressor and expansion work that the heat pump operates at the lowest. After this point, by increasing the discharge pressure, COP improves. It is noteworthy that, the enlarging pressure ratio amplifies the temperature differences in the expander that might risk entering the sub-critical zone(equation 24).

Recalling Figure 1, point 4 which is obtained by isentropic expansion at low stream pressure must be greater than the critical point which is 31 °C at 73 bar. The impact of pressure scale-up on the heat exchanger surface can be also discussed.

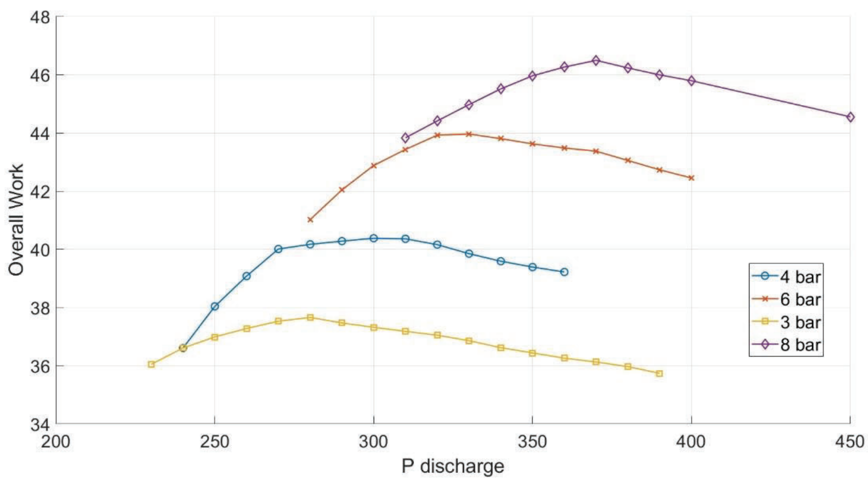

Figure 6. The effect of discharge pressure on the performance of sCO_2HP for various steam pressure

4. Conclusion

This work investigated a heat pump cycle undergoing a reverse Brayton cycle. CO_2 has been selected as the working fluid that entirely remains in the super-critical zone. The mathematical model has been created in the MATLAB Simulink environment. The heat pump model has been used as a steam generator to provide heat demand in diverse industry sectors. The maximum steam temperature is obtained at 180 °C which is evidently higher than available commercial models as well as any CO_2-based heat pump. In contrast with the available CO_2 heat pump model, it has been attempted to increase as much as possible the pressure ratio to increase the temperature profile. In this way, the internal heat exchanger unit has been replaced with an expansion device to recover mechanical work. As a result of this intervention, the performance of the machine improved and COP in the range of 1.57 up to 2.51 was obtained.

After that, the impact of the pinch point between CO_2 and steam on the performance of the heat pump was investigated. By increasing the pinch point, the overall surface required for heat

https://doi.org/10.52202/077185-0181

exchangers tends to decrease. However, a higher flow rate of CO_2 is demanded. The COP, in this case, improves slightly.

The sensitivity analysis on the effect of pressure increase demonstrated a non-linear correlation with the turbo machinery parts of the system. This is due to the non-linear thermodynamic properties of CO_2 in the super-critical zone that varies sharply. By increasing the pressure at the upstream side, the size of both the expander and compressor tends to reduce. However, the overall work to be inserted reaches its maximum value and it reduces afterwards. As a consequence, the COP of the machine initially reduces to reach its minimum value and then rises again.

The economic model is created as well to estimate the investment cost. The turbo-machinery parts are responsible for more than 60 % of the capital cost. The impact of discharge pressure on the final cost has been evaluated. By increasing the discharge pressure, turbomachinery and heat exchangers exhibit divergent trends: one increases while the other decreases. The optimal size, from an economic perspective, can be determined by analyzing these opposing trends.

REFERENCES

Ahmadi, M. H., Ahmadi, M. A., Pourfayaz, F., & Bidi, M. (2016). Thermodynamic analysis and optimization for an irreversible heat pump working on reversed Brayton cycle. *Energy Conversion and Management*, *110*, 260–267. https://doi.org/10.1016/j.enconman.2015.12.028

ARERA. (n.d.). *ARERA - Prezzi e tariffe*. https://www.arera.it/it/prezzi.htm#

Arpagaus, C., Bless, F., Uhlmann, M., Schiffmann, J., & Bertsch, S. S. (2018). High temperature heat pumps: Market overview, state of the art, research status, refrigerants, and application potentials. *Energy*, *152*, 985–1010. https://doi.org/10.1016/j.energy.2018.03.166

Bi, Y., Chen, L., & Sun, F. (2010). Exergetic efficiency optimization for an irreversible heat pump working on reversed Brayton cycle. *Pramana - Journal of Physics*, *74*(3), 351– 363. https://doi.org/10.1007/s12043-010-0032-9

Cao, F., Ye, Z., & Wang, Y. (2020). Experimental investigation on the influence of internal heat exchanger in a transcritical CO2 heat pump water heater. *Applied Thermal Engineering*, *168*(July 2019). https://doi.org/10.1016/j.applthermaleng.2019.114855

Chen, Y., & Gu, J. (2005). The optimum high pressure for CO2 transcritical refrigeration systems with internal heat exchangers. *International Journal of Refrigeration*, *28*(8), 1238–1249. https://doi.org/10.1016/j.ijrefrig.2005.08.009

Cho, S. K., Bae, S. J., Jeong, Y., Lee, J., & Lee, J. I. (2019). Direction for high-performance supercritical CO2 centrifugal compressor design for dry cooled supercritical CO2 Brayton cycle. *Applied Sciences (Switzerland)*, *9*(19). https://doi.org/10.3390/app9194057

Deng, N., Jing, X., Cai, R., Gao, J., Shen, C., Zhang, Y., & Sui, H. (2019). Molecular simulation and experimental investigation for thermodynamic properties of new refrigerant NBY-1 for high temperature heat pump. *Energy Conversion and Management*, *179*(October 2018), 339–348. https://doi.org/10.1016/j.enconman.2018.10.076

Fernandez, N., Hwang, Y., & Radermacher, R. (2010). Comparison of CO2 heat pump water heater performance with baseline cycle and two high COP cycles. *International Journal of Refrigeration*, *33*(3), 635–644. https://doi.org/10.1016/J.IJREFRIG.2009.12.008

Gilbert, T., Menon, A. K., Dames, C., & Prasher, R. (2023). Heat source and applicationdependent levelized cost of decarbonized heat. *Joule*, *7*(1), 128–149. https://doi.org/10.1016/j.joule.2022.11.006

IEA, Industrial energy consumption by fuel in the Net Zero Scenario, 2000-2030, IEA, Paris https://www.iea.org/data-and-statistics/charts/industrial-energy-consumption-by-fuelin-the-net-zero-scenario-2000-2030, IEA. Licence: CC BY 4.0. (n.d.). *IEA (2021), Electricity Information: Overview, IEA, Paris https://www.iea.org/reports/electricity-information-overview, License: CC BY 4.0*. (n.d.).

Jiang, J., Hu, B., Wang, R. Z., Deng, N., Cao, F., & Wang, C. C. (2022). A review and perspective on industry high-temperature heat pumps. *Renewable and Sustainable Energy Reviews*, *161*(March). https://doi.org/10.1016/j.rser.2022.112106

Kabat, N., Jende, E., Nicke, E., & Stathopoulos, P. (2023). Investigation on Process Architectures for High-Temperature Heat Pumps Based on a Reversed Brayton Cycle. *Proceedings of the ASME Turbo Expo*, *5*, 1–10. https://doi.org/10.1115/GT2023-102497

Kim, M. H., Pettersen, J., & Bullard, C. W. (2004). Fundamental process and system design issues in CO2 vapor compression systems. *Progress in Energy and Combustion Science*, *30*(2), 119–174. https://doi.org/10.1016/J.PECS.2003.09.002

Kim, S. G., Kim, Y. J., Lee, G., & Kim, M. S. (2005). The performance of a transcritical CO2 cycle with an internal heat exchanger for hot water heating. *International Journal of Refrigeration*, *28*(7), 1064–1072. https://doi.org/10.1016/J.IJREFRIG.2005.03.004

Klein, S. A., Reindl, D. T., & Brownell, K. (2000). Refrigeration system performance using liquid-suction heat exchangers. *International Journal of Refrigeration*, *23*, 588–596. www.elsevier.com/locate/ijrefrig

https://doi.org/10.52202/077185-0181

Klute, S., Budt, M., van Beek, M., & Doetsch, C. (2024). Steam generating heat pumps – Overview, classification, economics, and basic modeling principles. *Energy Conversion and Management*, *299*(November 2023). https://doi.org/10.1016/j.enconman.2023.117882

Liew, P. Y., & Walmsley, T. G. (2016). Heat pump integration for total site waste heat recovery. *Chemical Engineering Transactions*, *52*(2003), 817–822. https://doi.org/10.3303/CET1652137

Lo Basso, G., Mojtahed, A., Mario Pastore, L., & De Santoli, L. (2023). High-efficiency solution for an open-loop desiccant assisted solar cooling system by integrating transcritical CO2 heat pumps: A comprehensive techno-economic assessment. *Energy Conversion and Management: X*, *20*(August), 100437. https://doi.org/10.1016/j.ecmx.2023.100437

Lo Basso, G., Santoli, L. De, Paiolo, R., & Losi, C. (2020). *The potential role of transcritical CO 2 heat pumps within a solar cooling system for building services: The hybridised system energy analysis by a dynamic simulation model*. https://doi.org/10.1016/j.renene.2020.09.098

Madsboell, H., Weel, M., & Kolstrup, A. (2015). Development of a water vapor compressor for high temperature heat pump applications. *Refrigeration Science and Technology*, *c*, 1613–1620. https://doi.org/10.18462/iir.icr.2015.0845

Martins, G. L. (2016). Axial Turbine Cascade Correlation. *Applied Sciences (Switzerland)*, *6*(12). https://doi.org/10.3390/app6120420

Patel, V. K., & Raja, B. D. (2019). A comparative performance evaluation of the reversed Brayton cycle operated heat pump based on thermo-ecological criteria through many and multi objective approaches. *Energy Conversion and Management*, *183*(December 2018), 252–265. https://doi.org/10.1016/j.enconman.2018.12.109

Rony, R. U., Yang, H., Krishnan, S., & Song, J. (2019). Recent advances in transcritical CO 2 (R744) heat pump system: A review. In *Energies* (Vol. 12, Issue 3). https://doi.org/10.3390/en12030457

Tao, Y. B., He, Y. L., Tao, W. Q., & Wu, Z. G. (2010). Experimental study on the performance of CO2 residential air-conditioning system with an internal heat exchanger. *Energy Conversion and Management*, *51*(1), 64–70. https://doi.org/10.1016/J.ENCONMAN.2009.08.024

Techno-economic evaluation of combining heat pump and mechanical steam compression for the production of low pressure steam from waste heat - HPT - Heat Pumping Technologies. (n.d.). Retrieved February 10, 2024, from https://heatpumpingtechnologies.org/publications/techno-economic-evaluation-ofcombining-heat-pump-and-mechanical-steam-compression-for-the-production-of-lowpressure-steam-from-waste-heat/

The Future of Heat Pumps. (2022). *The Future of Heat Pumps*. https://doi.org/10.1787/2bd71107-en

Van de Bor, D. M., & Infante Ferreira, C. A. (2013). Quick selection of industrial heat pump types including the impact ofthermodynamic losses. *Energy*, *53*, 312–322. https://doi.org/10.1016/j.energy.2013.02.065

Wu, D., Hu, B., & Wang, R. Z. (2019). Theoretical and experimental investigation on a very high temperature heat pump with water refrigerant. *Refrigeration Science and Technology*, *2019-Augus*, 4502–4510. https://doi.org/10.18462/iir.icr.2019.0778

Xu, X., Hwang, Y., & Radermacher, R. (2010). *Refrigerant injection for heat pumping / air conditioning systems : Literature review and challenges discussions ` ne dans les syste ` mes a ` pompe a ` chaleur Injection du frigorige ´ rature et de conditionnement d ' air : passage en revue de la litte ´*. *4*. https://doi.org/10.1016/j.ijrefrig.2010.09.015

Yan, H., Wang, R., Du, S., Hu, B., & Xu, Z. (2021). Analysis and Perspective on Heat Pump for Industrial Steam Generation. *Advanced Energy and Sustainability Research*, *2*(5), 1– 11. https://doi.org/10.1002/aesr.202000108

Yang, D., Song, Y., Cao, F., Jin, L., & Wang, X. (2016). Theoretical and experimental investigation of a combined R134a and transcritical CO2 heat pump for space heating. *International Journal of Refrigeration*, *72*, 156–170. https://doi.org/10.1016/J.IJREFRIG.2016.07.016

Yu, X., Zhang, Y., Deng, N., Chen, C., Ma, L., Dong, L., & Zhang, Y. (2014). Experimental performance of high temperature heat pump with near-azeotropic refrigerant mixture. *Energy and Buildings*, *78*, 43–49. https://doi.org/10.1016/j.enbuild.2013.12.065

Zhang, J. F., Qin, Y., & Wang, C. C. (2015). Review on CO2 heat pump water heater for residential use in Japan. *Renewable and Sustainable Energy Reviews*, *50*, 1383–1391. https://doi.org/10.1016/j.rser.2015.05.083

Zhang, J., Meerman, H., Benders, R., & Faaij, A. (2020). Technical and economic optimization of expander-based small-scale natural gas liquefaction processes with absorption precooling cycle. *Energy*, *191*. https://doi.org/10.1016/j.energy.2019.116592

Zhang, Y., Peng, M., Xia, G., Wang, G., & Zhou, C. (2020). Performance analysis of S-CO2 recompression Brayton cycle based on turbomachinery detailed design. *Nuclear Engineering and Technology*, *52*(9), 2107–2118. https://doi.org/10.1016/j.net.2020.02.016

Zhu, W., Ren, X. D., Li, X. S., & Gu, C. W. (2018). Analysis and improvement of a twostage centrifugal compressor used in an MW-level gas turbine. *Applied Sciences (Switzerland)*, *8*(8). https://doi.org/10.3390/app8081347

Zhu, Y., Huang, Y., Li, C., Zhang, F., & Jiang, P. (2018). *Experimental investigation on the performance of transcritical CO 2 ejector – expansion heat pump water heater system Compressor Oil return line Oil separator Ejector Receiver Fan heater*. *167*(April), 147– 155.

https://doi.org/10.52202/077185-0181